Supplementary Information (SI) for Dalton Transactions.
This journal is © The Royal Society of Chemistry 2024

Electronic supplementary information for:

Cascaded Utilization of Magnetite Nanoparticles@Onion-Like Carbons from Wastewater Purification to Supercapacitive Energy Storage

Authors

Xin Jiao,[a,b,c,d,e] *Min Xiao,*[a,b,c,d] *Fengshi Cai,*[a,b,c,d] *Yingchun Fan,*[a,b,c,d] *Shuaipeng Meng,*[a,b,c,d] *Xiude Guan,*[e] *Huiquan Wang,*[a,b,c,d] *Chenguang Zhang*[a,b,c,d]*

Affiliations

[a] School of Materials Science and Engineering, Tianjin University of Technology, Tianjin 300384, PR China.

[b] Institute for Green Nanotechnology, Tianjin University of Technology, Tianjin 300384, PR China.

[c] Tianjin Key Laboratory for Photoelectric Materials & Devices, Tianjin University of Technology, Tianjin 300384, PR China.

[d] Key Laboratory of Display Materials and Photoelectric Devices, Tianjin University of Technology, Ministry of Education, Tianjin 300384, PR China.

[e] College of Materials Engineering, Shanxi College of Technology, Shuozhou, Shanxi Province 036000, PR China.

Corresponding author:

Email: cgzhang@tjut.edu.cn (Chenguang Zhang).

Supplementary figures

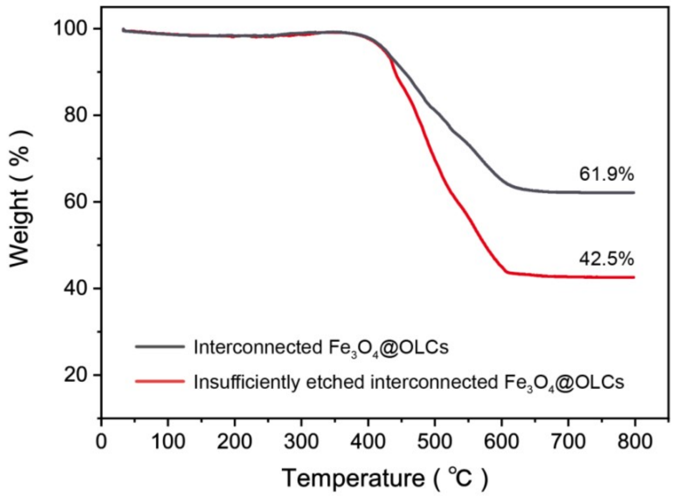

Fig. S1. TG curves of interconnected Fe_3O_4@OLCs and insufficiently etched interconnected Fe_3O_4@OLCs at a heating rate of 10 ℃ min^{-1} from 30 to 800 ℃ in air.

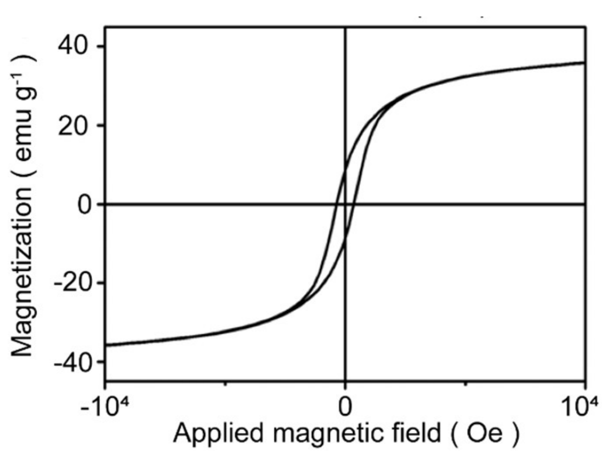

Fig. S2. Magnetic hysteresis loop of insufficiently etched interconnected Fe_3O_4@OLCs.

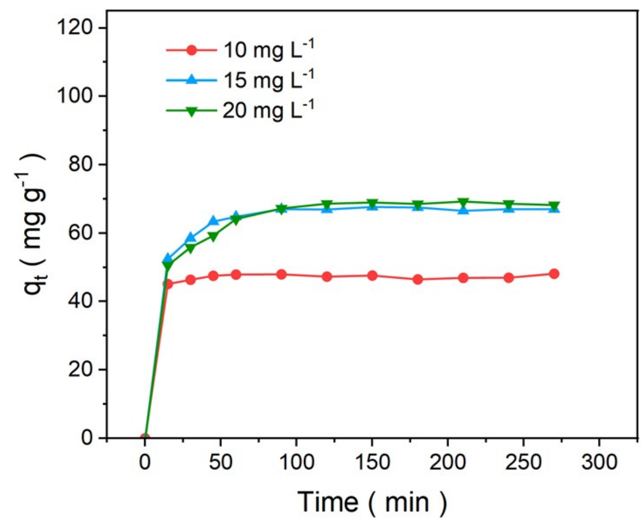

Fig. S3. Variation of the adsorption capacities of interconnected Fe_3O_4@OLCs with treated period.

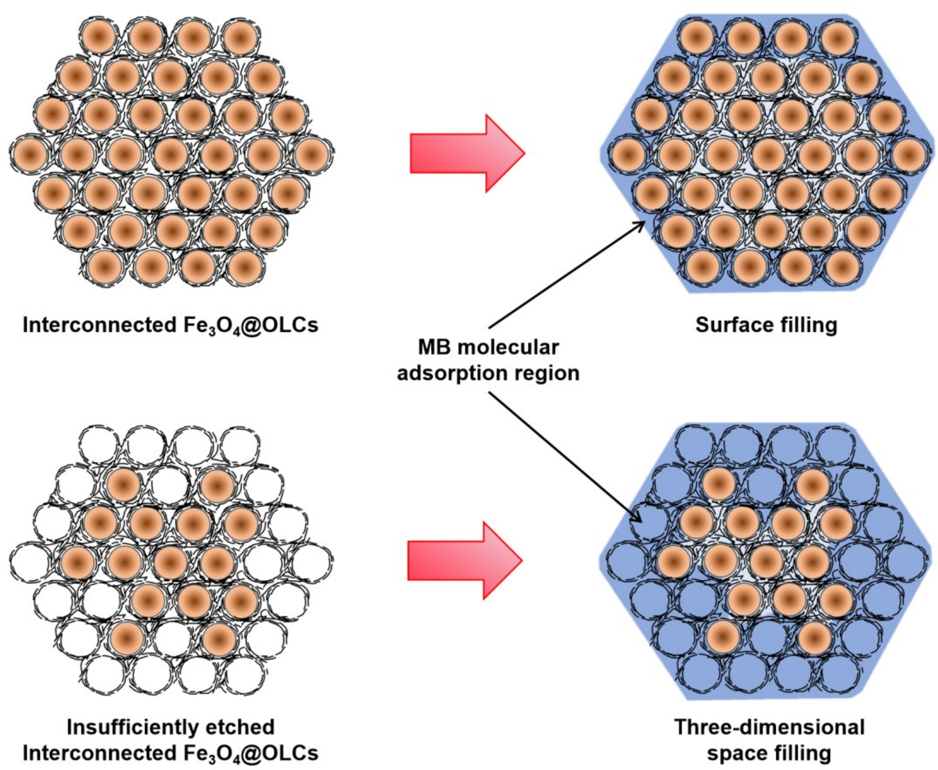

Fig. S4. Schematic illustration of the difference in MB adsorption mechanisms between interconnected Fe_3O_4@OLCs and insufficiently etched interconnected Fe_3O_4@OLCs.

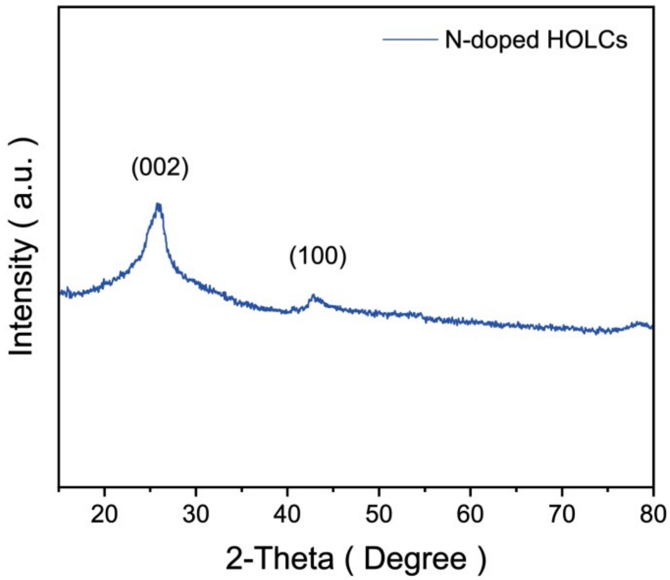

Fig. S5. XRD profile of the N-doped HOLCs.

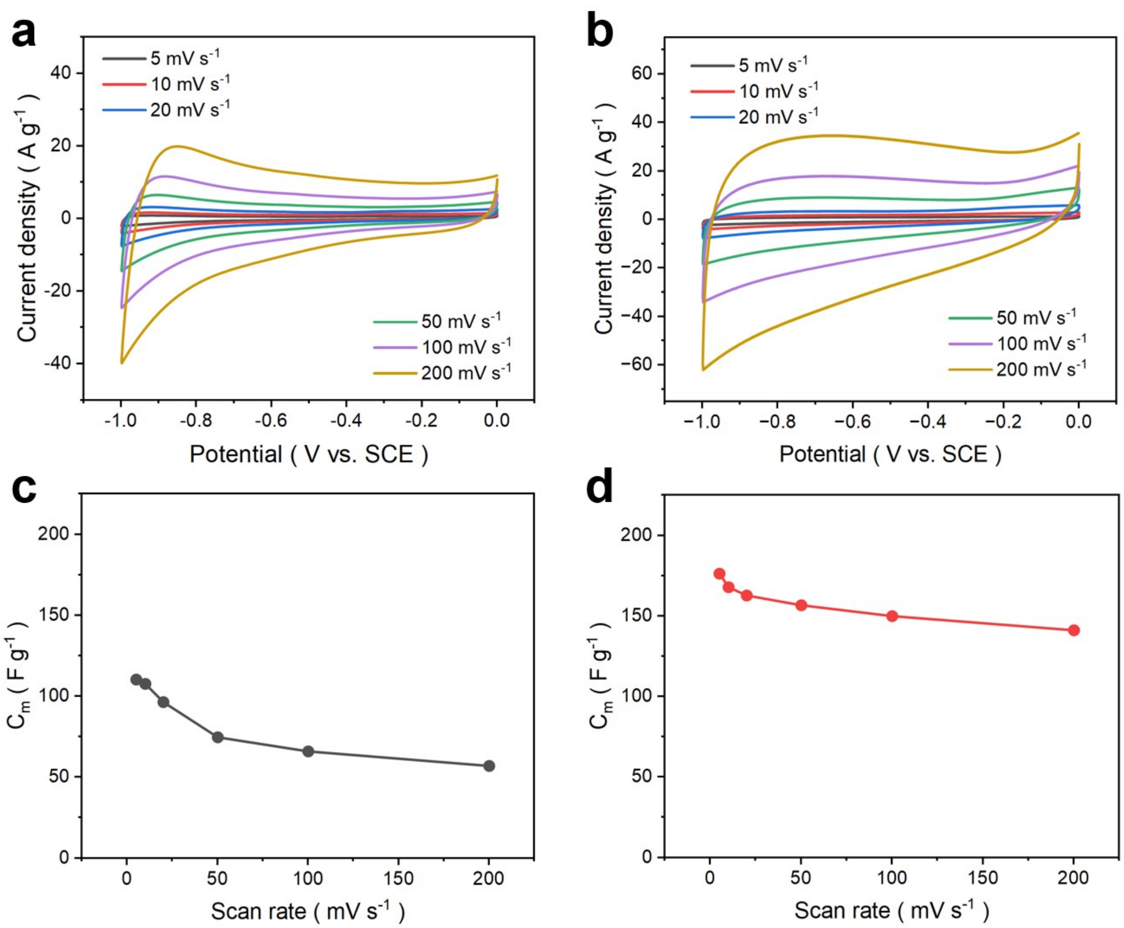

Fig. S6. CV curves of (a) insufficiently etched interconnected Fe_3O_4@OLCs and (b) N-doped porous carbon structure at different scan rates from 5 to 200 mV s^{-1} in three-electrode testing system. Specific gravimetric capacitances (C_m) calculation results of (c) Fe_3O_4@OLCs and (d) N-doped HOLCs at different scan rates from 5 to 200 mV s^{-1}.

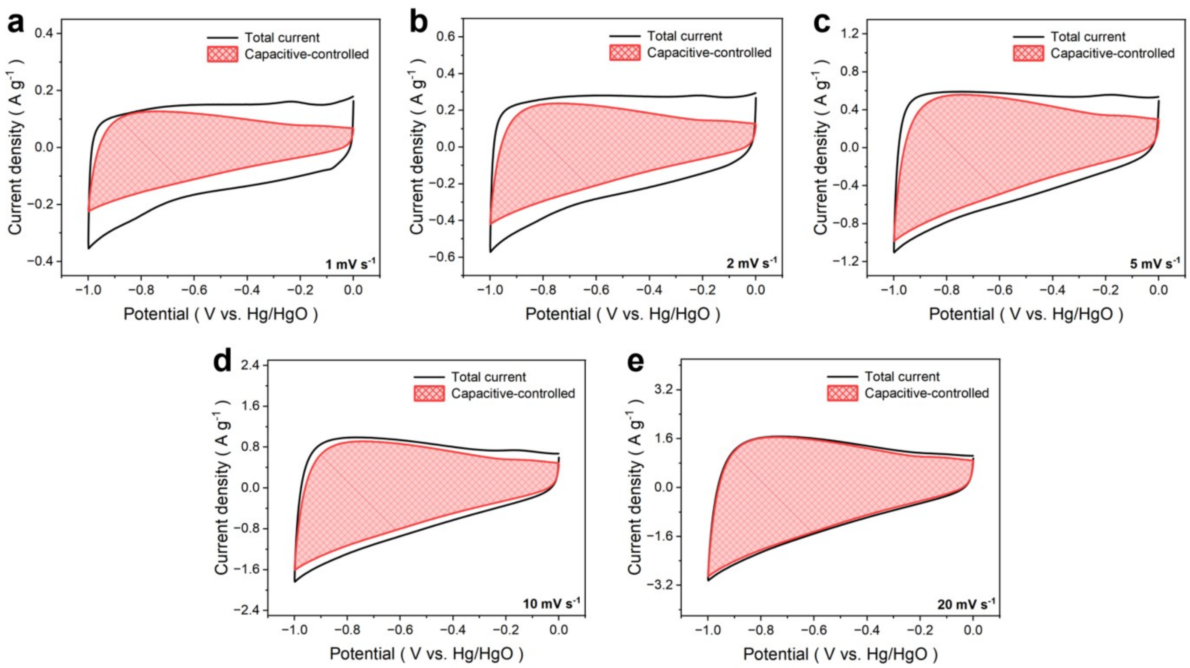

Fig. S7. Electrochemical kinetic analysis of N-doped HOLCs. Percentage of capacitive-controlled charge contribution from EDLC based on CV measurements at scan rates of (a) 1, (b) 2, (c) 5, (d) 10 and (e) 20 mV s^{-1}.

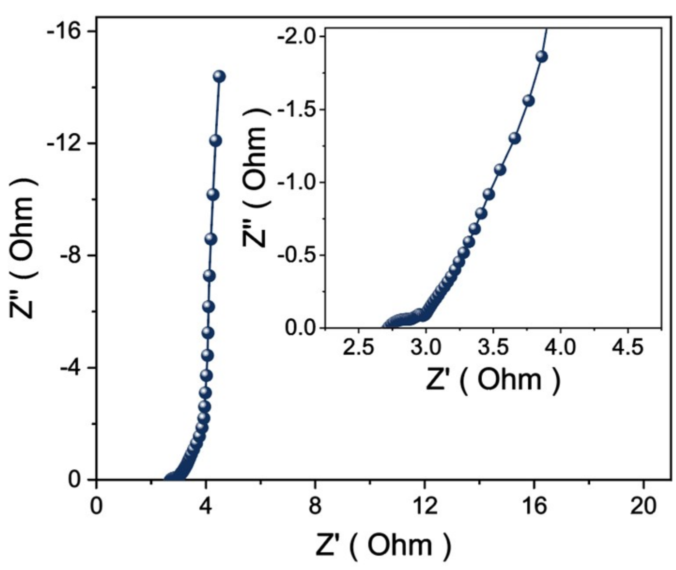

Fig. S8. Nyquist plot of supercapacitor.

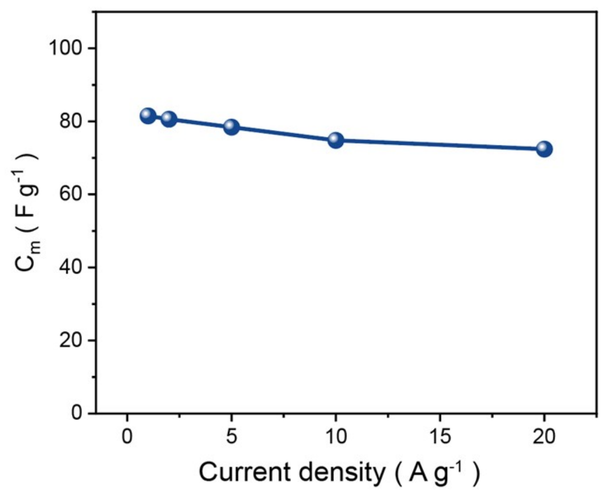

Fig. S9. Specific gravimetric capacitances (C_m) versus current densities of the supercapacitor device.

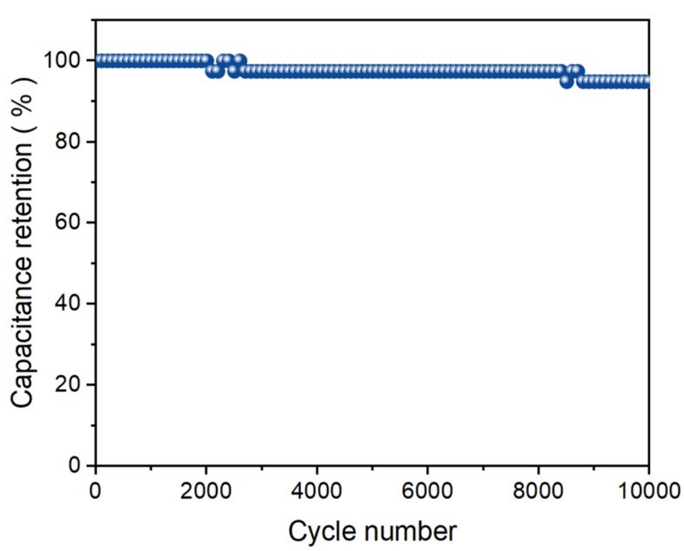

Fig. S10. Cycling stability of supercapacitor measured at a charging-discharging current density of 10 A g^{-1}.

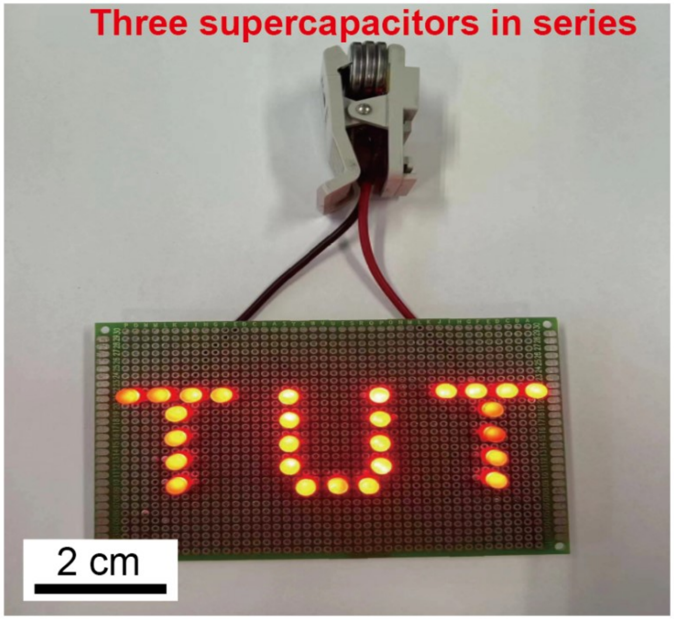

Fig. S11. 27 red LEDs powered by three supercapacitors connected in series.

Table S1. Comparisons of energy storage performances of supercapacitor based on N-doped HOLCs with other carbon-based supercapacitors.

Materials	Electrolyte	Energy density (Wh kg^{-1})	Power density (kW kg^{-1})	Cycle stability	Ref.
Sulfur-doped carbon nano-onions	1M Na_2SO_4	10.6	0.1	95% after 10000 cycle	S1
Quinone-decorated onion-like carbon	1M H_2SO_4	6.4	19.2	90% after 10000 cycle	S2
Nori:$ZnCl_2$-2:1	6M KOH	6.1	0.05	96% after 5000 cycle	S3
ZIF-8 derived carbon	6M KOH	4.66	0.21	96% after 10000 cycle	S4
HPCF	6M KOH	9.1	3.5	95% after 10000 cycle	S5
PANI-carbon nanotube composites	H_2SO_4/PVA	5.8	1.1	83.2% after 2000 cycle	S6
TPI-P-700	1M H_2SO_4	10.5	0.5	100% after 10000 cycle	S7
Phosphorus-doped porous carbon	1M H_2SO_4	10.6	0.22	98.3% after 5000 cycle	S8
HPCSLS-700	7M KOH	8.6	0.014	92% after 10000 cycle	S9
N-C-HPCS	6M KOH	6.1	0.25	108% after 10000 cycle	S10
N-doped HOLCs	3M KOH	11.3 7.9	0.51 8.9	94.6% after 10000 cycle	This Work

Reference:

S1. G. Dhakal, D. Mohapatra, T.L. Tamang, M. Lee, Y.R. Lee, J.-J. Shim, Energy, 2021, **218**, 119436.

S2. M. Bhaumik, K. Raju, I. Arunachellan, T. Ludwig, M.K. Mathe, A. Maity, S. Mathur, Electrochim. Acta, 2020, **342**, 136111.

S3. B. Li, F. Dai, Q. Xiao, L. Yang, J. Shen, C. Zhang, M. Cai, Energy Environ. Sci., 2016, **9**, 102-106.

S4. H. N. Abdelhamid, S. A. Al Kiey, W. Sharmoukh, Appl. Organomet. Chem., 2021, **36**, 1.

S5. Y. Zhang, R. Shao, W. Xu, J. Ding, Y. Wang, X. Yan, W. Shi, M. Wang, Chem. Eng. J., 2021, **419**, 129576.

S6. Y. Wang, S. Tang, S. Vongehr, J. A. Syed, X. Wang, X. Meng, Scientific Reports 2016, **6**, 12883.

S7. D. Yan, Y. Wu, R. Kitaura, K. Awaga, J. Mater. Chem. A, 2019, **7**, 26829-26837.

S8. G. Lin, Q. Wang, X. Yang, Z. Cai, Y. Xiong, B. Huang, RSC Adv. 2020, **10**, 17768.

S9. J. Pang, W. Zhang, J. Zhang, G. Cao, M. Han, Y. Yang, Green Chem., 2017, **19**, 3916-3926.

S10. S. Park, B. Seo, D. Shin, K. Kim, W. Choi, Chem. Eng. J., 2022, **433**, 134486.